Precipitation of Ferrites in Nafion® Membranes

LOUISE RAYMOND,[1] J.-F. REVOL,[1] D. H. RYAN,[2] and R. H. MARCHESSAULT[1,*]

[1]Pulp and Paper Research Centre and Chemistry Department, McGill University, 3420 University Street, Montreal, Quebec H3A 2A7, and [2]Physics Department, McGill University, 3600 University Street, Montreal, Quebec H3A 2T8, Canada

SYNOPSIS

Iron oxide particles were precipitated in Nafion® 117 perfluorinated ion-exchange membranes using four different methods. Precipitated ferrites yielded magnetically responsive nanocomposite films and probed structural variations in the membrane. Optical microscopy, transmission electron microscopy, vibrating sample magnetometry (VSM), and Mössbauer spectroscopy were used to characterize the materials. Microscopy showed that the ferrites were distributed unevenly across the films with a dense skin making up the surface layers. Higher temperature enhanced accessibility to iron and increased ferrite loadings were obtained for these samples. Nanosize particles of magnetite (Fe_3O_4) were present as disks or as clusters of disks in all the treated films. Needles and bundles of needles of maghemite (γ-Fe_2O_3) were produced in the films that were reacted at the boil. All the samples exhibited superparamagnetic response by VSM. Due to the shorter time scale of the Mössbauer measurement ($\sim 10^{-7}$ s), ferrimagnetic response was detected for boiled and autoclaved samples. © 1996 John Wiley & Sons, Inc.

INTRODUCTION

Nanocomposite materials based on cellulosic substrates, such as wood pulp and sodium carboxymethylcellulose crosslinked pulp, have been reported.[1,2] An *in situ* synthesis of ferrites was used to prepare these cellulosic nanocomposites. This approach biomimicked magnetic bacteria[3-6] that intracellularly biomineralize ferrites of very small size ($\sim$ 500 Å). Nanocomposites are of growing interest because of the unique magnetic, electrical, and optical properties exhibited by particles of nanoscale dimensions.[7] Magnetically responsive cellulosic fibers containing superparamagnetic ferrites, have potential applications in security paper and as magnetic filters for biotechnological separations and air purification. A process using an ion-exchange step to transfer ferrous ions into the cellulosic cell wall was followed by precipitation of ferrous hydroxide (alkali treatment) and oxidation to create superparamagnetic magnetite (Fe_3O_4) and maghemite (γ-Fe_2O_3).[2] Similar reaction schemes have been used to synthesize superparamagnetic particles in synthetic ion-exchange resins for magnetic xerographic toners.[8-10]

For comparison with our work using wood pulp,[2] a perfluorinated ion-exchange membrane (Nafion® 117, Du Pont) was chosen for this study to examine the influence of its homogeneous chemical composition on the distribution of precipitated ferrites. Nafion® 117 has a similar equivalent weight of sulfonic acid groups as the sulfonated thermomechanical wood pulp used previously.[2] It is also hydrophilic but much less swellable in water at room temperature than the wood pulp. The uniformity of clusters of sulfonic acid groups in this membrane was expected to prevent surface deposition of ferrites, as was observed for the microfibrillar wood pulp.[2]

Nafion® products are generally prepared by copolymerizing tetrafluoroethylene with a perfluorovinyl ether sulfonyl fluoride to form a melt-processable polymer that is extruded and hydrolyzed.[11] The result is an ionomer composed of a polytetrafluoroethylene backbone with pendant sulfonic acid

* To whom correspondence should be addressed.

Journal of Applied Polymer Science, Vol. 59, 1073–1086 (1996)
 CCC 0021-8995/96/071073-14

groups on perfluorinated ether side chains. Nafion® has been used as a separation membrane in electrochemical cells, particularly by chlor-alkali producers, because of its exceptional chemical, thermal, and electrical stability in addition to good ionic conductivity and permselectivity.[12,13] It is used as a superacid solid catalyst for acylation, alkylation, alcohol dehydration, esterification, and nitration,[13,14] and as a metal-cation exchanged Lewis acid for the alkylation of aromatics.[15] Techniques such as small-angle neutron[16,17] and X-ray scattering,[16,18–20] Mössbauer spectroscopy[21–24] and extended X-ray absorption of fine structure (EXAFS)[22] have been used to probe the molecular architecture of the membrane. The microstructure of this membrane has been the topic of much debate,[16–20] but it is generally accepted that ion-rich regions (clusters) exist in a hydrophobic backbone matrix.

Nanocomposite materials are often prepared by synthesizing small particles ($\sim$ 100 Å) in polymer resins that have a morphology that provides particle size control.[8–10] For example, monodispersed silver particles (20–30 Å) have been grown and oxidized in Nafion® films by ion exchange and reduction of the Ag(I) form of the membrane, followed by exposure to oxygen.[25] Iron oxide[26] and iron hydroxides[23] have also been synthesized in Nafion® membranes using standard ion-exchange and precipitation methods. In this study iron oxide particles were precipitated *in situ* in a Nafion® 117 membrane by four different approaches. The nanocomposite films were characterized using four major techniques: optical microscopy, transmission electron microscopy (TEM), vibrating sample magnetometry (VSM), and Mössbauer spectroscopy. Structural variations inside the membrane seemed to be replicated by the distribution of ferrites: the "skin" of the membrane was found to be more loaded with ferrite as opposed to the membrane interior.

EXPERIMENTAL

Materials and Functional Group Quantification

Nafion® 117, a 0.007-in. thick perfluorinated membrane (Du Pont), was purchased from Aldrich Chemical Co. This transparent film is hygroscopic in nature, therefore, it was stored in its sealed package in a dessicator. An equivalent weight analysis of 1.100 eq/kg of material was provided by Aldrich.

Conductometric titration, according to a previously published methodology,[27,28] was used to quantify the number of sulfonic acid groups. Approximately 1 g of the film, as purchased in protonated form, was cut into 2 × 2 cm squares and stirred in a 0.001*M* NaCl solution, to create a Donnan equilibrium.[29] The automated burette added 0.5 mL of 0.100*M* NaOH titrant every 10 min. The membrane was found to contain 1.05 ± 0.04 eq/kg of sulfonic acid groups, in good agreement with the supplier's analysis.

In Situ Syntheses

Method A: In Situ *Method Using Oxygen Gas as Oxidant*

Approximately 1 g of the film was cut into 2 × 2 cm squares and stirred in 100 mL of 0.01 g/mL of $FeCl_2 \cdot 4H_2O$ solution for 3 days, changing the solution daily.[15] The colorless films turned a transparent yellow with time. Ferrous hydroxide was precipitated by the addition of 50 mL of 0.100*M* NaOH. The films turned a transparent greenish-black color. The suspension was heated to 65° ± 5°C in a water bath and oxygen was bubbled through the suspension at a rate of 6 mL/min for 2 h.[1,2] The films turned a transparent ruby-red color during this period. The material was cycled through the reaction five times with a square of sample collected after each cycle. The samples were washed several times by stirring vigorously in deionized water. The cycling, collection, and washing steps were performed for the four different methods of ferrite synthesis.

Method B: In Situ *Method Using Hydrogen Peroxide as Oxidant*

The same procedure as in method A was used with the exception of the oxidation step: 100 mL of a 10% hydrogen peroxide solution was added to the suspension over a period of 30 min, followed by stirring for 3 h at room temperature. The oxidized films were a deeper ruby-red than those obtained from the method described in method A. This color deepened upon cycling, reflecting higher iron loadings.

Method C: Synthesis at Boil

The film squares were boiled for 1 h in 100 mL of 0.01 g/mL of $FeCl_2 \cdot 4H_2O$ solution. The films turned a deep, transparent yellow over this period. Precipitation of ferrous hydroxide was achieved by immersing the films in 50 mL of boiling 0.100*M* NaOH with stirring for 1 h. The films at this time were an opaque greenish-black color. Hydrogen peroxide was

added as in method B, but at the boil. The oxidized films turned an opaque reddish-black color.

Method D: Autoclaving

The film squares were placed in 100 ml of $FeCl_2 \cdot 4H_2O$ (0.01 g/mL) solution, covered, and autoclaved in a Model 9000-D autoclave, Napco E series, for 1 h (130°C, 23 psi). The films turned a deep, transparent yellow after this step. The films were then transferred into 50 mL of 0.100 *M* NaOH and autoclaved again for 1 h. The opaque greenish-black films were then oxidized as in method C. The oxidized films were an opaque rusty-brown color with some visible dark brown streaking.

Swelling Measurements

The degree of swelling of the Nafion® film, after each stage of the various treatments, was measured by comparing the average thickness (t) of a film square with the measured thickness of a dried (t_d) piece of film oven-dried overnight at 70°C.[30] Squares of film were removed after each step of the treatments, blotted between absorbent papers, and the thickness was measured at 10 different places along the film with a micrometer to within three decimal places (±0.005 mm) and averaged. The ratio of the difference in thickness between the two ($t - t_d$) and the thickness of the dried piece of film (t_d), multiplied by 100, gave the percentage increase in the thickness (±2%) of the membrane. This value was used as a measure of the degree of swelling of the film.

VSM

The magnetic properties of the Nafion® films were studied using VSM. A small strip of film was cut (~15 mg), folded, and placed in the sample holder. The materials were vibrated within a magnetic field of up to 1.5 T at room temperature. The response of the materials (magnetization) was obtained as a function of the applied magnetic field.

TEM and Ultrathin Sectioning

TEM was performed on thin sections of Nafion® after one, three, and five cycles of each of the treatments. For sectioning, thin strips of film were cut from the treated Nafion® film squares and placed in propylene oxide overnight to dehydrate the material. The films were embedded in a Spurr resin cured at 70°C overnight. Ultrathin sectioning of the resulting blocks was performed with a Reichert Ultracut E microtome equipped with a diamond knife. The TEM instrument was a Philips EM 400 operated at 120 kV for imaging by diffraction contrast in the bright field mode and for selected area (SA) electron diffraction.

Optical Microscopy

A Nikon microphot-FXA optical microscope (Nikon Corporation) was used to measure the thickness of the skin layer of all Nafion® samples. Sections (12 μm) were cut with a glass knife from the blocks of embedded samples prepared for TEM, and mounted onto glass slides. The relative skin thickness was calculated by measuring the average skin thickness (cf. Fig. 1: thickness of the dark surface layer of the Nafion® film) and dividing by the average width of the section (cf. Fig. 1: width of the section where the embedding process has not swollen the section).

Energy-Dispersive X-Ray Spectrometry

The microtomed sections were mounted on Cu grids for TEM. Energy-dispersive X-ray spectrometric (EDS) microanalysis was used to determine the iron and sulfur distribution across a Nafion® membrane. The ultramicrotome sections were examined using an analytical electron microscope (Philips CM30) at an accelerating voltage of 100 kV with an X-ray energy-dispersive spectrometer (Link AN10/85S system) equipped with an ultrathin window, allowing the analysis of light elements down to boron. Measurements were made in the TEM imaging mode with a focused 80-nm diameter electron probe. Spectra were acquired in about 300 s.

Mössbauer Spectroscopy

Mössbauer spectra were recorded at room temperature with a conventional constant-acceleration spectrometer in transmission geometry using a 1 Gbq $^{57}CoRh$ source. Spectra were obtained for the films after one, three, and five cycles of each treatment. Low temperature Mössbauer measurements were performed on one sample using a Mössbauer cryostat (Janis Research Company, Inc.) for temperatures from room temperature down to 80 K, and an APD Cryogenics Inc. HC-2 fridge for measurements in the 11–60 K range. One to three layers of film were mounted onto the spectrometer. The

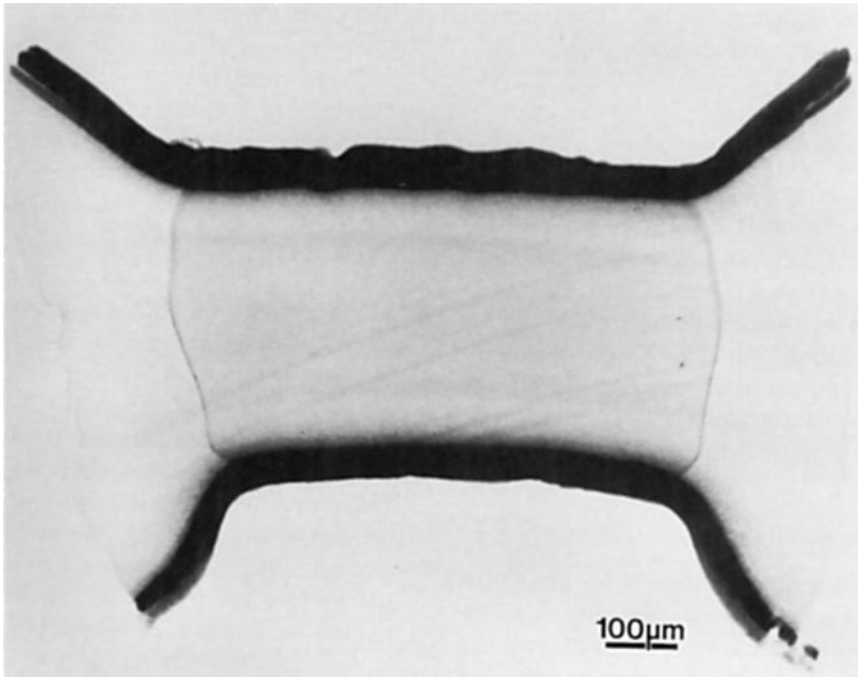

Figure 1 Optical micrograph of a section of Nafion® film after three cycles of boiling (method C). The skin is seen as the dark band. The left and right sides of the section are swollen during the embedding process.

spectra were fitted using a standard Mössbauer computer fitting program.

RESULTS AND DISCUSSION

Optical Microscopy

Figure 1 is an optical micrograph of a section of Nafion® following three cycles of method C. The dark border indicates that the skin of the Nafion® film is highly loaded with iron, whereas the interior region of the material appears less dense. The left and right sides of the section show where the film has been swollen during the embedding process. Sections for TEM were cut mainly from these swollen areas to minimize chattering of the diamond knife through the sample.

The skin thickness, as a function of the method of sample treatment and iron content, was measured using optical microscopy (see Experimental). A plot of relative skin thickness as a function of method and iron loading is shown in Figure 2. The skin thickness is shown to vary with the method of ferrite synthesis and iron content. At approximately 2% iron, methods A and B show similar ranges of penetration, whereas methods C and D result in skin thicknesses two to three times larger. This is an effect of the higher temperature conditions of methods C and D that promotes swelling of the skin (see swelling discussion). The iron content of these samples increases with cycling without an increase in skin thickness. The skin layer seems to have been swollen to its maximum capacity after one cycle of higher temperature treatment. Method B shows an increase in skin thickness with iron content. A maximum of 10% of the film seems to be occupied by a highly accessible skin layer.

Transmission Electron Microscopy

Figure 3 shows a TEM micrograph of a section of Nafion® after five cycles of the *in situ* reaction using oxygen as the oxidant (method A). A skin of uniformly distributed disklike ferrites, having an average size of 200 Å, is observed. Inside the film (right side of the micrograph), the concentration of iron decreases sharply to smaller particles less than 100 Å in size. The ferrites having disklike morphology were identified by electron diffraction as magnetite (Table I). Magnetite was present in all of the treated films as disks or as clusters of disks. The clusters,

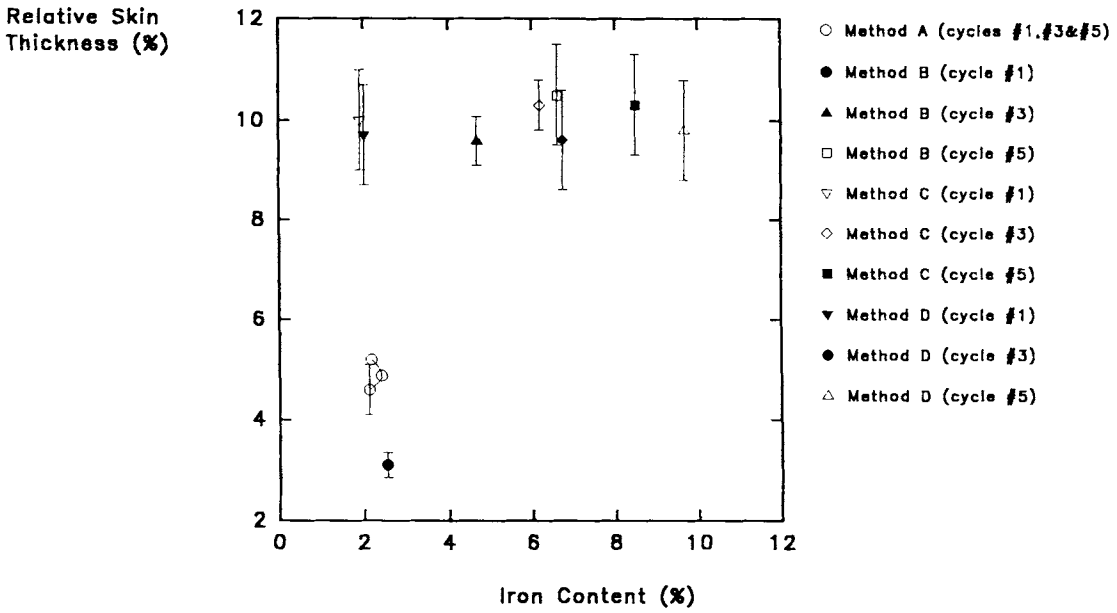

Figure 2 Relative skin thickness as a function of method of sample treatment and iron content. A maximum of 10% of the material is occupied by the skin.

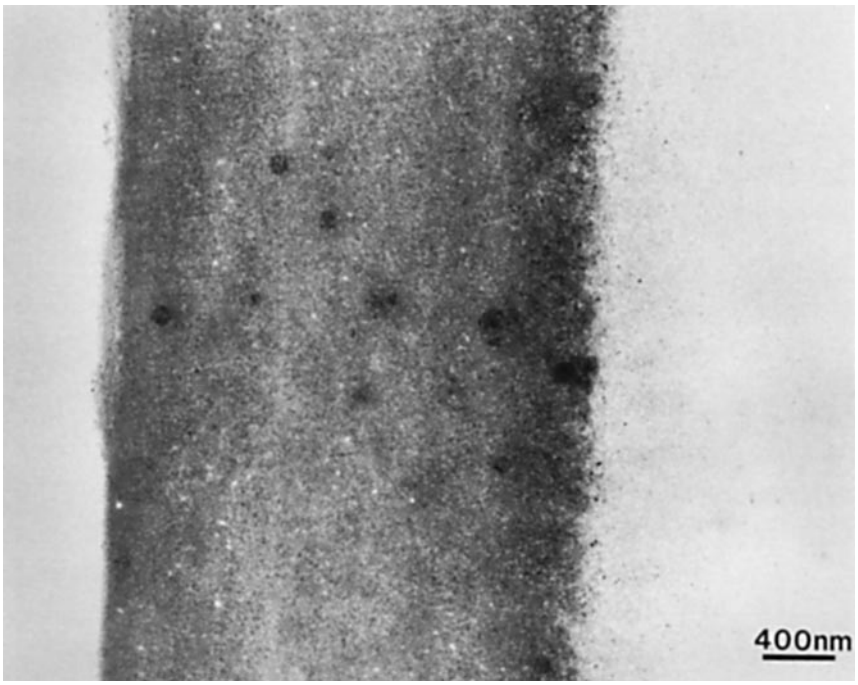

Figure 3 TEM micrograph of a section of Nafion® after five cycles of the *in situ* reaction using oxygen as the oxidant (method A). The skin of the film is seen at the left side of the micrograph and is loaded with ferrites (Fe_3O_4) approximately 200 Å in size. A lower concentration of smaller ferrites extends into the interior of the film (right side of the micrograph).

Table I Electron Diffraction Data (*d* Spacings/Å) for Magnetite (Fe_3O_4) Synthesized *In Situ* Using Nafion® after One Cycle of Method B

In Situ Ferrites	XRD[31]
2.82	2.860
2.38	2.439
2.01	2.022
1.59	1.650
1.54	1.557
1.41	1.429

on average, were comprised of less than 10 aggregated disks.

Films treated as in methods B, C, and D display ferrite density fluctuations across the skin of the sections. A typical example of this is seen from TEM micrographs of the first and fifth cycle Nafion® samples oxidized with peroxide (method B). A section of the first cycle sample (Fig. 4) shows the skin composed of several layers having different iron concentrations. The average iron profile across this sample was studied using EDS, confirming the presence of a higher concentration in the skin. A uniform distribution of sulfur across the membrane was also observed for this sample. Disks less than 60 Å in size are visible at the exterior surface of the film (top of the micrograph). The size of the disks increases to about 400 Å as the interior of the film is approached, with the ferrites being most concentrated at the interior border of the skin. The membrane interior (very low iron concentration) is composed primarily of a dispersion of disks that range from 25 to 60 Å in size and clusters of disks that average 100 Å in size.

Figure 5 shows dramatic fluctuations in ferrite concentration across the skin after the fifth cycle of method B. Disks approximately 60 Å in size are concentrated at the surface (left side of the micrograph) and increase in size to about 300 Å as the skin is penetrated. The interior (right-hand side of the micrograph) is composed mainly of uniformly distributed disks having an average size of about 80 Å. The fifth cycle peroxide-treated sample contains 6.61% iron versus 2.54% iron for the first cycle sample. It appears that iron deposits unevenly and a layered structure is produced with cycling. Heterogeneity in fine structure seems to account for the observed layering of iron distribution: porous skin layers over a dense core. The latter develops only fine ferrites extending from the interior border of the skin. This

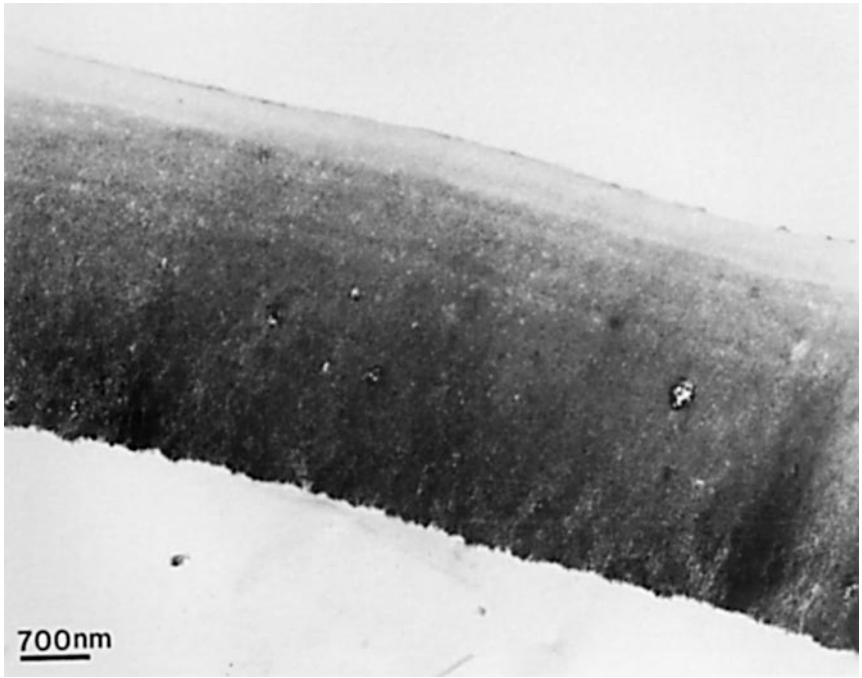

Figure 4 TEM micrograph of a section of Nafion® film after one cycle of method B. The skin of the film is seen at the top of the figure and is layered with a gradient of increasing iron concentration.

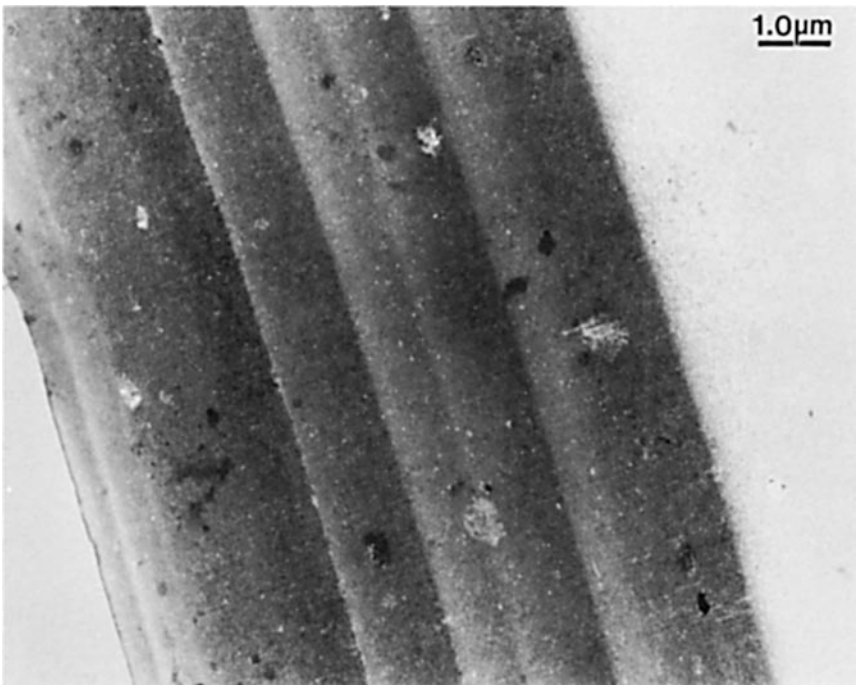

Figure 5 TEM micrograph of a section of Nafion® film after five cycles of method B. The skin of the film (left side of the micrograph) has more pronounced layering of ferrite distribution than seen in Figure 4.

overall structure is mirrored on the other side of the membrane. Morphological differences arising from quenching and calendering effects of the melt-extrusion process[11] could explain the observed layered structure.

Figure 6 is a TEM micrograph of a section of Nafion® film after one cycle of boiling (method C). Higher temperature treatment of the film produced greater accessibility, resulting in increased ferrite loadings for the higher cycle samples (Table II), while still retaining the skinlike structure. Changes in ferrite morphology and size are observed across the film. The skin, shown at the left side of the micrograph, shows a pronounced gradient of ferrites having disklike morphology, ranging from 20 to 300 Å in size. A small concentration of clusters of disks (less than 600 Å) and needles (~ 600 Å long × 60 Å thick) is found adjacent to the border of the skin. Large bundles, approximately 3500 Å in size, of needles form a layer at the edge of the skin, extending to widely distributed disklike ferrites (~ 160 Å) in the interior shown at the right side of the micrograph. TEM of sections of the material after three and five cycles of reaction demonstrated that the concentration and size of the ferrites increase upon cycling, with a higher concentration of iron remaining in the skin. A second layer of bundles of needles is formed following three cycles. Most notable is that high temperature treatment removes the layering feature of the skin (cf. Fig. 5).

The TEM micrographs of the boiled samples confirm that the skin of the membrane is porous and more accessible to iron than the interior. This morphological feature may be related to the manufacturing conditions used (melt extrusion).[11] The needlelike ferrites, identified as γ-Fe_2O_3 by electron diffraction (Table III), were produced from boiling due to an increase in rate of oxidation under these conditions. The deposition of needles and bundles of needles in the inner skin (i.e., boundary between the skin and the film interior) of the membrane is probably due to higher accessibility of this area.

Figure 7 is a section of film after one cycle of autoclaving (method D), showing similar characteristics to the boiled films (method C). A larger concentration of 100-Å disklike ferrites and 300-Å clusters of disks is visible in the skin shown at the bottom of the micrograph. The size of the clusters increases to about 500 Å as the interior layer is approached (top of the micrograph). Bundles, approximately 4500 Å in size, of needles border the interior layer composed of widely distributed needles (~ 600

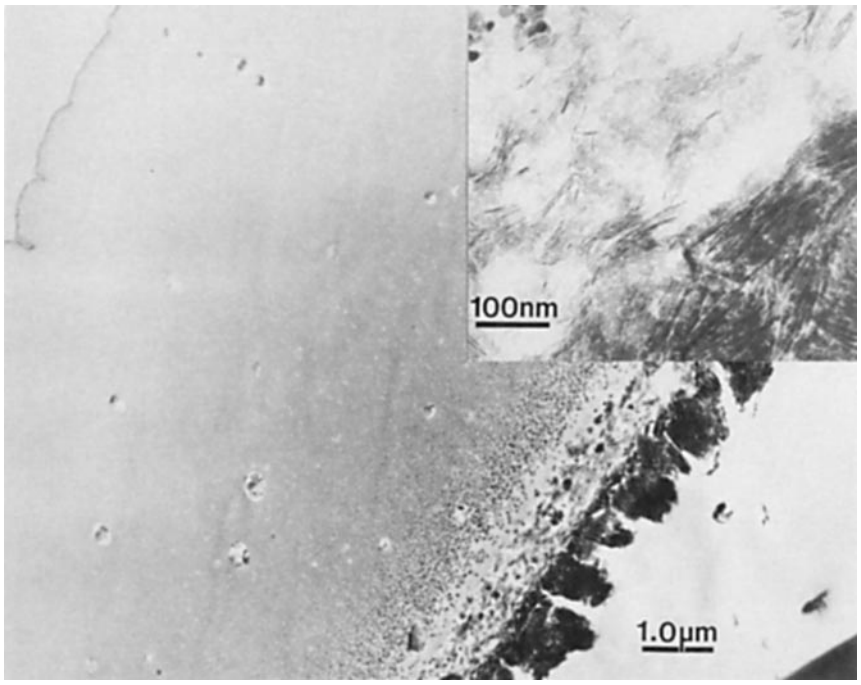

Figure 6 TEM micrograph of a section of Nafion® film after one cycle of boiling (method C), showing the skin of the film at the top left of the micrograph. Bundles, approximately 3500 Å in size, of needles form a layer in the inner skin of the film (right side of the micrograph). Inset: higher magnification of the needle-bundle layer (γ-Fe_2O_3).

Å long × 60 Å thick) and disks (less than 300 Å) and aggregates of both oxides. TEM of sections of film after three and five cycles show (as seen for the boiled samples) an increase in size and concentration of ferrite. Two and three layers of needle bundles were observed for the third and fifth cycle samples, respectively.

The accessibility, or swellability, of the films was measured using the increase in thickness of the film following the various stages of the treatments (see Experimental). It was found that during the steps of the oxygen and peroxide treatments, the films increased approximately 10% in thickness, as they do at room temperature in deionized water. Boiling brought about an increase of about 20% in thickness and autoclaving showed the highest increase (~ 30%). Increased iron loadings for the higher cycle boiled and autoclaved samples were observed due to greater accessibility of the membrane under higher temperature conditions. Larger disklike ferrites, as well as bundles of needlelike ferrites, were precipi-

Table II Iron Composition of Nafion® Film as a Function of Treatment and Number of Reaction Cycles

	Cycle (%Fe)		
Method	1	3	5
A	2.12	2.41	2.17
B	2.54	4.68	6.61
C	1.92	6.18	8.48
D	2.02	6.73	9.67

The iron composition (±1%) of the samples was determined by digesting a weighed sample in an acid mixture and analyzing spectrometrically using atomic absorption.

Table III Electron Diffraction Data (*d* Spacings/Å) for Maghemite (γ-Fe_2O_e) Synthesized *In Situ* Using Nafion® after One Cycle of Method D

In Situ Ferrites	XRD[31]
4.11	4.180
2.44	2.519
2.27	2.230
2.13	2.079
1.64	1.609
1.42	1.480
1.19	1.205
1.07	1.087

tated in the skin of the film under these conditions, probably as a result of larger pores arising from swelling. This might account for the removal of the layering feature of the skin with higher temperature. Uniformly distributed clusters of disks were observed in the skin of the autoclaved samples (cf. Fig. 7), possibly for the same reasons.

Magnetic Properties

VSM showed that all of the materials were superparamagnetic in character, showing no hysteresis, remanence, or coercivity. Superparamagnetic materials are easily magnetized in a magnetic field but do not retain magnetization once removed from the field. The magnetization curves for the films treated as in method A are shown in Figure 8. Disklike ferrites in the 100–200 Å size range and a low iron concentration (Table II) for these samples produced a magnetic response that was rather noisy. The saturation magnetization was estimated to be about 0.25 J/T/kg. Figure 9 shows the magnetization curves for the samples oxidized using peroxide (method B). Higher saturation values than the oxygen-treated samples were obtained. The first cycle sample saturates at about 0.3 J/T/kg, increasing to 0.7 J/T/kg for the fifth cycle sample.

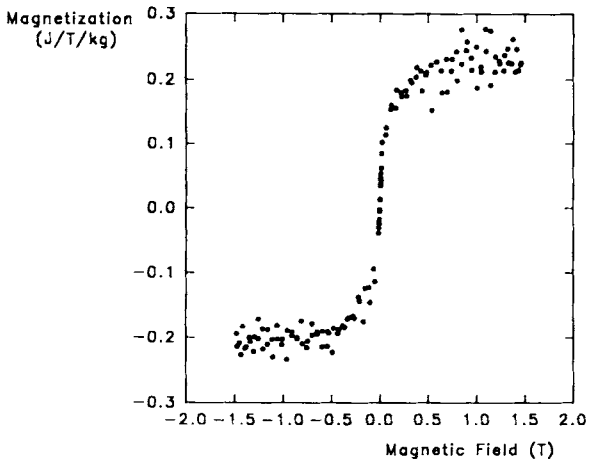

Figure 8 Magnetization curves for the Nafion® film treated as in method A. All cycle samples are superparamagnetic.

Figure 10 shows that the samples prepared using method C exhibit superparamagnetic behavior, while having greater saturation than the materials treated as in methods A and B. The fifth cycle sample con-

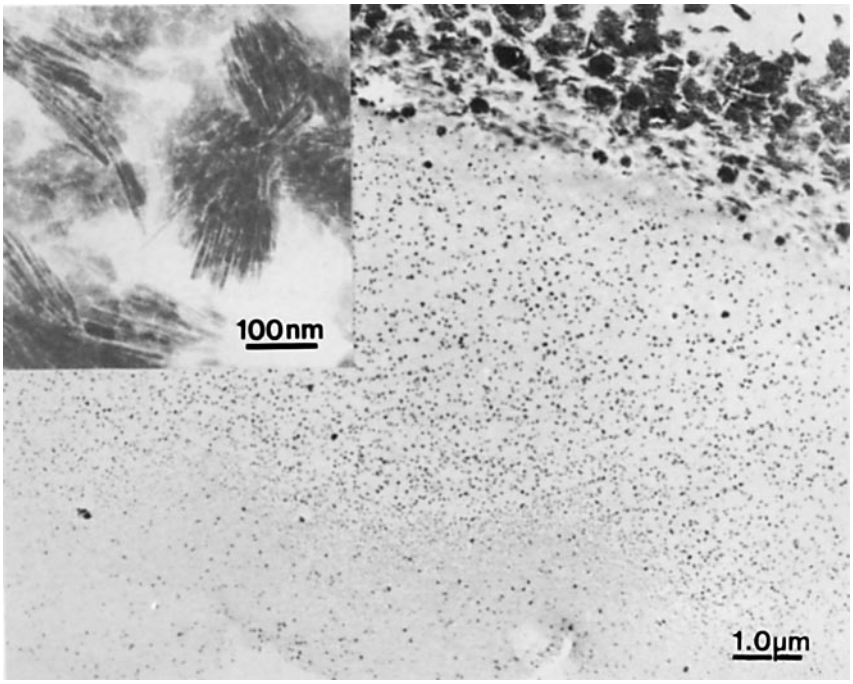

Figure 7 TEM micrograph of a section of Nafion® film after one cycle of autoclaving (method D). Disks and clusters of disks are present in the skin (bottom of the micrograph), in addition to a layer of bundles of needles adjacent to the border of the interior (top of the micrograph). Inset: higher magnification of the clusters of disks and bundles of needles.

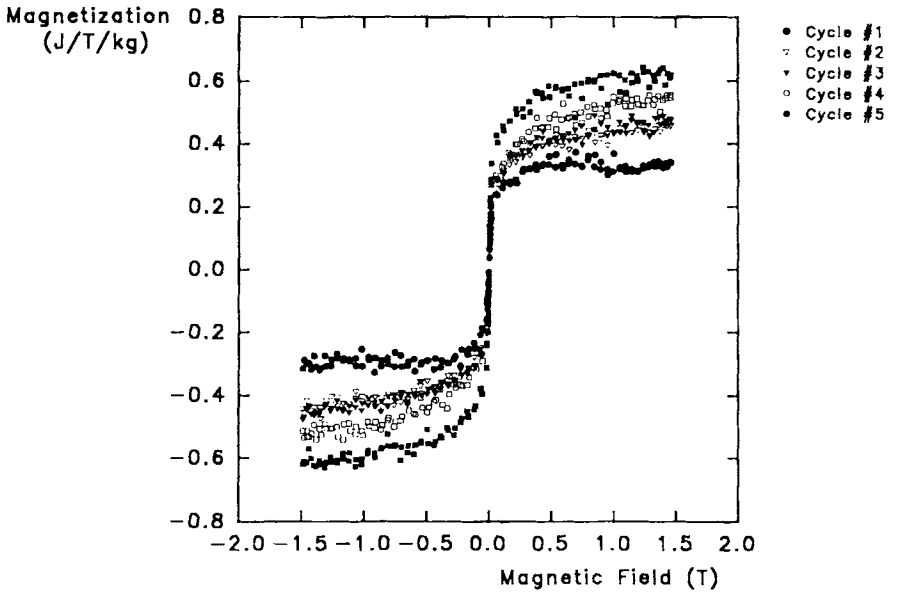

Figure 9 Magnetization curves for the Nafion® film treated as in method B. A small increase in saturation magnetization is observed with cycling and all the samples are superparamagnetic.

tains 8.48% iron and saturates at a value of about 6 J/T/kg. The autoclaved materials (method D, Fig. 11) exhibit similar magnetic behavior and have comparable iron contents (Table II) to the boiled samples. The magnetization curves show that all the autoclaved samples have lower saturation values than the boiled samples.

Information on the average particle size can be obtained from the magnetization data by converting the measurements to joules/tesla/kilogram of iron using the iron contents given in Table II. Because the small superparamagnetic particles of magnetite respond more weakly to an applied field than larger particles, the same amount of magnetite in fine par-

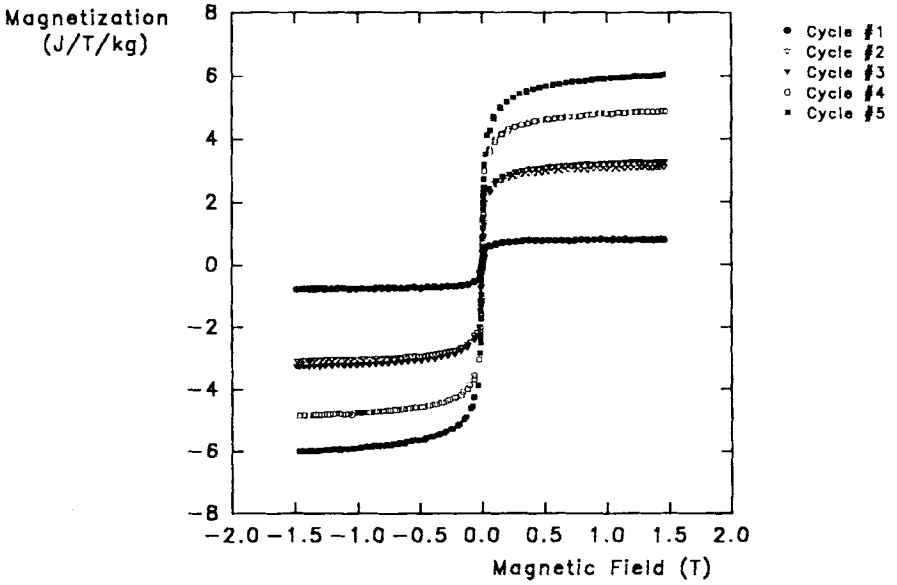

Figure 10 Magnetization curves for the Nafion® film treated as in method C. The samples are superparamagnetic and have higher saturation values than the samples prepared using methods A and B.

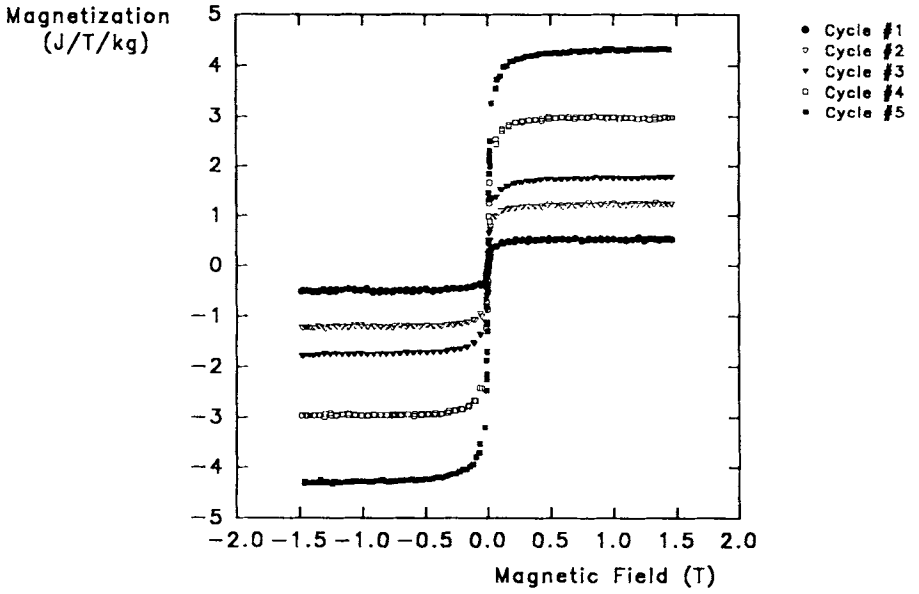

Figure 11 Magnetization curves for the Nafion® film treated as in method D. These samples exhibit similar behavior to the boiled films, although less saturation is observed for all cycles.

ticle form will give a lower magnetization than that in the form of coarser particles. The results in Figure 12 show that for methods A and B, the magnetization is small and cycle independent indicating that the iron is deposited as quite fine particles and that the particles do not grow on cycling, results that are in agreement with the TEM data presented. By contrast, methods C and D exhibit much larger magnetizations that also show marked increases on cycling, reflecting initial deposition of larger particles and their subsequent growth on cycling, observations that are again consistent with the earlier TEM data. While it is clear that methods C and D lead to larger particles, they are still in the superparamagnetic regime as the observed magnetization falls short of the saturation value of 124 J/T/kg of iron for bulk magnetite.

Mössbauer spectroscopy was used to study the magnetic properties of the treated films and for characterization purposes. The time scale of the Mössbauer measurement ($\sim 10^{-7}$ s) allowed the detection of static magnetic components not detectable by the magnetic measurement (VSM) that has a seconds time scale. Spectra of samples prepared by methods A and B were paramagnetic, reflecting the very fine particles present; all samples prepared by methods C and D showed an additional magnetically ordered component from particles large enough to appear blocked at room temperature. Typical spectra obtained after cycle 3 for each method are shown in Figure 13. Samples prepared by methods A and B showed only the paramagnetic component at all stages, confirming the TEM and magnetization observation of no particle growth in materials prepared by these methods. The ordered component in the spectra of samples prepared by methods C and D increases relative to the paramagnetic part on cy-

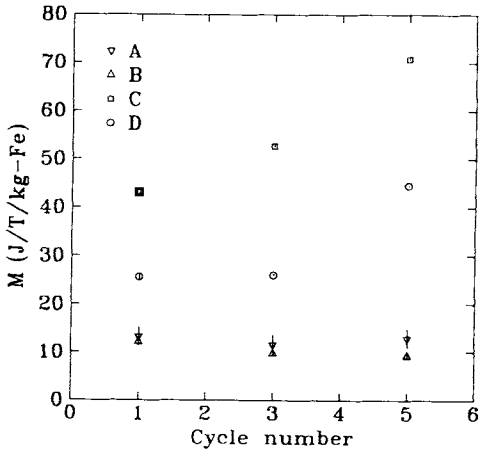

Figure 12 Magnetization in J/T/kg of iron as a function of cycle number and method of treatment. Samples prepared by methods C and D show increases in magnetization with cycling, indicating increasing particle size.

cling, providing further evidence of particle growth during cycling.

The fifth cycle sample of the peroxide-treated film (method B) was chosen for a blocking temperature study, because this sample seemed to have a relatively narrow particle size distribution and an iron content high enough for sufficient absorption. Figure 14 shows a series of Mössbauer spectra at different temperatures. A gradual development of the magnetic sextet, characteristic of magnetite, was observed as the temperature was decreased. The area of the paramagnetic peak (±10%) was plotted as a function of temperature in Figure 15. An oversimplification would suggest that there are two blocking temperatures at approximately 290 and 125 K, indicating that roughly two size populations are present. It appears from this plot that approximately 30% of the particles appear large and 70% small. Comparison with TEM data (cf. Fig. 5) shows that this is not unreasonable because disks of about 60–80 Å in size are present in the skin and also in the interior of the film. Larger disklike ferrites (~ 300 Å) predominate in the inner skin. The relative proportions of magnetite and maghemite were not quantifiable because the sample blocks below the Verwey† transition of magnetite (between 110 and 120 K).[32]

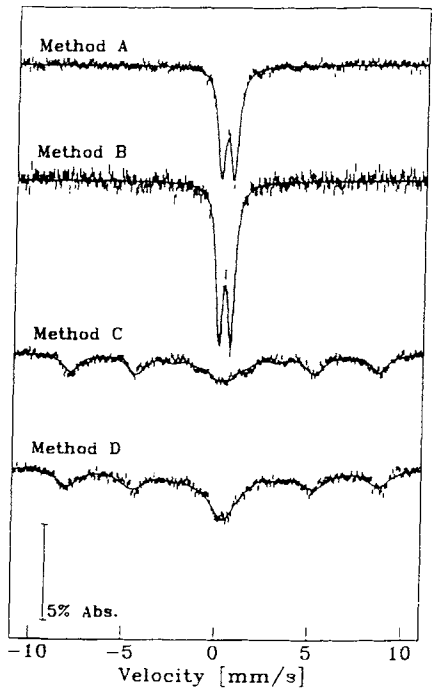

Figure 13 Room temperature Mössbauer spectra of the Nafion® film after three cycles of treatment for all methods. Samples prepared using methods A and B show 100% paramagnetic behavior, whereas those prepared using methods C and D have a ferrimagnetic component.

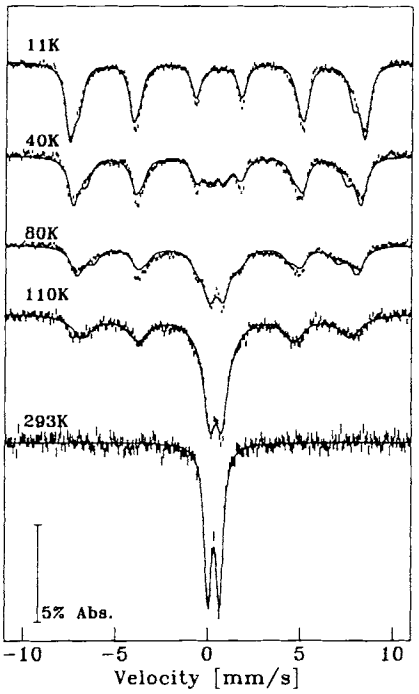

Figure 14 Low temperature Mössbauer spectra of the Nafion® film treated as in method B, after five cycles of reaction. A gradual reduction of the paramagnetic component was observed with decreasing temperature.

CONCLUSIONS

It has been shown that magnetism can be easily induced in Nafion® membranes without compromising the physical integrity of the material. Methods A and B (low temperature) produced superparamagnetic films containing nanosize magnetite (Fe_3O_4) ranging from 25 to 300 Å in size. Higher temperature treatments (methods C and D) increased the size and concentration of ferrite in the films as a result of swelling. Needles and bundles of needles of maghemite (γ-Fe_2O_3) were precipitated under these conditions due to more rigorous oxidation. The presence of the membrane, during the synthesis of iron oxide, appears to influence the properties of the resulting particles: control experiments performed

† Verwey transition: Electron hopping occurs between Fe^{2+} and Fe^{3+} ions on the octahedral (B) sites in the magnetite structure below 120 K, producing a completely averaged spectrum. Spectra obtained below this temperature are complex.[3]

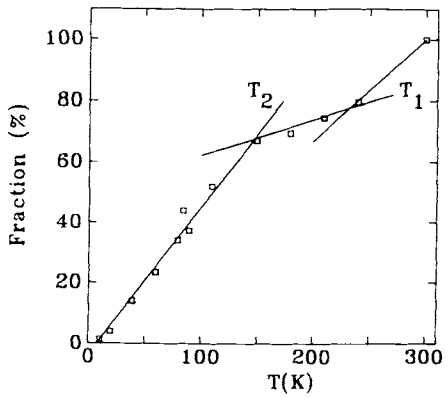

Figure 15 Area of the paramagnetic peak plotted as a function of temperature of the Nafion® film described in Figure 14. Roughly two particle size populations can be estimated from the curve.

without membrane showed the presence of nonmagnetic amorphous hydroxides that were larger than the nanoparticles precipitated *in situ*. Vibrating sample magnetometry detected superparamagnetic behavior for all Nafion® samples; the shorter time scale of the Mössbauer measurement enabled detection of ferrimagnetism for the samples prepared using methods C and D.

The precipitation of ferrites in Nafion® served to replicate the internal structure of the membrane. The distribution of iron was found to be uneven with a greater concentration at both surfaces, producing a skin effect for all treatments.[33] A layering texture was more pronounced for the lower temperature treatments. Higher temperature conditions decreased the layering deposition of the particles as a result of swelling, while still retaining the skin structure. The relative skin thickness was found to be a function of both iron content and method of treatment: a maximum of 10% of the film seems to be occupied by the skin layer. A structure having porous skin layers over a dense interior was implied. This morphological feature is probably related to the film manufacturing conditions used (melt extrusion).[11]

As shown from our studies with wood pulp fibers,[2] accessibility seemed to be a factor for the precipitation of ferrite, primarily at the surface of the fibers. This phenomenon was also observed for the Nafion® material, showing ferrites arranged in layers that are part of the skinlike structure of the melt-processed film. Recent work on wet-spun filaments of cellulose, which have a skin-core structure, produced a ferrite distribution similar to the Nafion® films.

Magnetized Nafion® could have applications as coatings for conductive oxide catalytic electrodes.[21] Uses for the superparamagnetic films in biotechnology for magnetic separations could be investigated due to the possibility of reuse of the material. The catalytic properties of these films have yet to be determined.

The authors would like to thank Louis Godbout of the Pulp and Paper Research Institute of Canada for guidance with the sectioning and Dr. Dorothea Wiarda of the Physics Department of McGill University for assistance with the Mössbauer instrumentation. This work was supported by the Natural Sciences and Engineering Research Council (Canada) and Xerox Corporation. Louise Raymond received a fellowship from the Quebec Ministry of Education and the Pulp and Paper Research Institute of Canada.

REFERENCES

1. R. H. Marchessault, S. Ricard, and P. Rioux, *Carbohydr. Res.*, **224,** 133 (1992).
2. L. Raymond, J.-F. Revol, D. H. Ryan, and R. H. Marchessault, *Chem. Mater.*, **6,** 249 (1994).
3. R. Blakemore, *Science,* **190,** 377 (1975).
4. R. B. Frankel, *Annu. Rev. Biophys. Bioeng.*, **13,** 85 (1984).
5. T. Matsunga and S. Kamiya, *Appl. Microbiol. Biotechnol.*, **26,** 328 (1987).
6. J. F. Stolz, S.-B. R. Chang, and J. L. Kirschvink, *Nature,* **321,** 849 (1986).
7. R. P. Andres, R. S. Averback, W. L. Brown, L. E. Brus, W. A. Goddard, A. Kaldor, S. G. Louie, M. Moscovits, P. S. Peercy, S. J. Riley, R. W. Siegel, F. Spaepen, and Y. Wang, *J. Mater. Res.*, **4**(3), 704 (1989).
8. R. F. Ziolo, U.S. Pat. 4,474,866 (1984) (to Xerox Corporation).
9. T. Smith and D. Wychick, *J. Phys. Chem.*, **84,** 1621 (1980).
10. R. F. Ziolo, E. P. Giannelis, B. A. Weinstein, M. P. O'Horo, B. N. Ganguly, V. Mehrotra, M. W. Russell, and D. R. Huffman, *Science,* **257,** 219 (1992).
11. W. Pusch and A. Walch, *Angew. Chem. Int. Ed. Engl.*, **21,** 660 (1982).
12. S. C. Stinson, *C&EN,* March 15, 22 (1982).
13. *Aldrichimica Acta,* **19,** 76 (1986).
14. G. A. Olah, G. K. Prakash, and J. Sommer, *Superacids,* Wiley, New York, 1985, p. 284.
15. F. J. Waller, *Br. Polym. J.*, **16,** 239 (1984).
16. P. Aldebert, B. Dreyfus, G. Gebel, N. Nakamura, M. Pineri, and F. Volino, *J. Phys. France,* **49,** 2101 (1988).
17. B. Dreyfus, G. Gebel, P. Aldebert, M. Pineri, M. Escoubes, and M. Thomas, *J. Phys. France,* **51,** 1341 (1990).

18. T. D. Gierke, G. E. Munn, and F. C. Wilson, *J. Polym. Sci.: Polym. Phys. Ed.,* **19,** 1687 (1981).
19. A. Eisenberg, B. Hird, and R. B. Moore, *Macromolecules,* **23,** 4098 (1990).
20. R. B. Moore, D. Bittencourt, M. Gauthier, C. E. Williams, and A. Eisenberg, *Macromolecules,* **24,** 1376 (1991).
21. B. Rodmacq, M. Pineri, J. M. D. Coey, and A. Meagher, *J. Polym. Sci.: Polym. Phys. Ed.,* **20,** 603 (1982).
22. H. K. Pan, D. J. Yarusso, G. S. Knapp, M. Pineri, A. Meagher, J. M. D. Coey, and S. L. Cooper, *J. Chem. Phys.,* **79,** 4736 (1983).
23. A. Meagher, B. Rodmacq, J. M. D. Coey, and M. Pineri, *Reactive Polym.,* **2,** 51 (1984).
24. J. M. D. Coey, in *Structure and Properties of Ionomers,* A. Eisenberg and M. Pineri, Eds., NATO Advanced Study Institute Series 198, D. Reidel Publishing Company, Dordrecht, 1987, p. 117.
25. G. D. Chryssikos, V. D. Mattera, Jr., W. M. Risen, Jr., and A. T. Tstsas, *J. Catalysis,* **93,** 430 (1985).
26. M. Pineri, J. C. Jesior, and J. M. D. Coey, *J. Membr. Sci.,* **24,** 325 (1985).
27. R. H. Marchessault, P. Rioux, and L. Raymond, *Polymer,* **33,** 4025 (1991).
28. L. Raymond, F. G. Morin, and R. H. Marchessault, *Carbohydr. Res.,* **224,** 133 (1992).
29. A. M. Scallan, Tappi J., **66,** 73 (1983); cf. also *J. Appl. Polym. Sci.,* **99,** 1554 (1980).
30. G. Gebel, P. Aldebert, and M. Pineri, *Polymer,* **34,** 333 (1993).
31. Powder Diffraction File, compiled by JCPDS International Centre for Diffraction Data, 1984.
32. N. N. Greenwood and T. C. Gibb, *Mössbauer Spectroscopy,* Chapman & Hall, Ltd., London, 1971, p. 252.
33. P. L. Shao, K. A. Mauritz, and R. B. Moore, *Chem. Mater.,* **7,** 192 (1995).

Received March 20, 1995
Accepted July 20, 1995